

Special
Collection

Synthesis and Characterization of Bis(pyridylimino)isoindolide Alkali Metal Complexes in Three Redox States

Jonas O. Wenzel,^[a] Israel Fernández,^[b] and Frank Breher*^[a]

Non-innocent ligands (NILs) like bis(pyridylimino)isoindolide (BPI) play crucial roles in coordination chemistry, biosciences, catalysis and material sciences. Investigating the isolated redox states of NILs is inevitable for understanding their redox-activity and fine-tuning the properties of corresponding metal complexes. The limited number of fundamental studies on the coordination behavior and redox chemistry of reduced BPI species is suggested to hamper further applications of the title compounds. This work describes for the first time the isolation of alkali metal complexes of BPI and Me₂BPI in three different

oxidation states and their characterization by means of NMR or EPR spectroscopy, DFT calculations, and SC-XRD studies. The latter revealed the connection between bond orders in the ligand scaffold and its oxidation state. The paramagnetic compound Me₂BPI-K₂ was isolated as a coordination copolymer with 18-crown-6, which enabled the characterization of the dianionic BPI radical. Furthermore, the so-far unknown trianionic state of BPI was reported by the isolation of BPI-K₃. This divulges an unprecedented bis(amidinato)isoindolide coordination mode.

Introduction

Ligands that prevent the exact determination of the oxidation state of metal ions are known as redox-active or non-innocent ligands (NILs).^[1] The utilization of NILs alters the redox levels of metal complexes compared to their redox inactive counterparts, which are dominated by the redox chemistry of the metal ions. Therefore, they are suggested to show high potential in coordination chemistry,^[2] catalysis,^[3] material sciences^[4] and life sciences, which is also signified by the various porphyrinoid NILs in biological systems.^[5]

Fine-tuning redox properties of metal complexes according to corresponding applications inevitably requires knowledge of the isolated redox chemistry of both the metal ion and the isolated pre-ligand. A famous monodentate representative for NILs is NO.^[6] Studying its redox activity is, for instance, directly connected to a deeper understanding of fundamental processes

in biochemistry.^[7] Also, bidentate NILs based on hetero-1,3-diene systems like catecholates,^[8] thioles,^[9] or diimines^[10] were investigated thoroughly, which has led to a good number of applications in small molecule activation,^[11] catalysis,^[12] or metal-organic frameworks,^[13] as well as to fundamental progress in artificial photosynthesis.^[14] Tridentate redox-active ligands belong to the class of pincer ligands and show strong binding affinities to metal ions due to the chelate effect. This often leads to highly stable molecular complexes with finely tunable redox properties making them superior in modern ligand design to low coordinating NILs.^[15] Redox-active bis(imino)pyridines, for example, revealed stable iron complexes in different oxidation states and enabled even reductive elimination of C–C bonds from Fe^{II}.^[16] Other tridentate NILs like substituted diphenylamines^[15] or dihydrazono-pyrroles^[17] did likewise show high potential in organometallic chemistry and homogeneous catalysis.

Bis(arylimino)isoindolides are also tridentate NILs with bis(pyridylimino)isoindolide (BPI) being the most famous representative of this family (Figure 1).^[22] Complexes of s-, p-, d-, and f-block elements were reported using BPI ligands and especially the transition metal complexes were discussed in the context of current chemical issues like redox flow batteries,^[18] homogeneous catalysis,^[21,23] living polymerization^[24] and water splitting.^[19,20] In most cases, the NH moiety of the central isoindoline scaffold is deprotonated making BPI a monoanionic NNN pincer ligand featuring a fully π -conjugated backbone (Figure 1). Unraveling the redox properties of preligands like BPI can be realized by isolating their alkali metal complexes as those metal ions are suggested to be fully redox innocent leading to essentially ligand-controlled redox chemistry. This approach was already realized for NILs like diimines^[25] or iminopyridines.^[26] The exploration of these reduced NILs unraveled completely new classes of coordination compounds

[a] J. O. Wenzel, Prof. Dr. F. Breher
Karlsruhe Institute of Technology (KIT)
Institute of Inorganic Chemistry (AOC)
Engesserstraße 15, 76131 Karlsruhe (Germany)
E-mail: breher@kit.edu
<http://www.aoc.kit.edu/breher/>

[b] Prof. Dr. I. Fernández
Universidad Complutense de Madrid
Departamento de Química Orgánica I
Facultad de Ciencias Químicas and Centro de Innovación en Química Avanzada (ORFEO-CINQA)
28040 Madrid (Spain)

Supporting information for this article is available on the WWW under <https://doi.org/10.1002/ejic.202300315>

Part of the Special Collection "Evolving with Inorganic Chemistry for 25 Years".

© 2023 The Authors. European Journal of Inorganic Chemistry published by Wiley-VCH GmbH. This is an open access article under the terms of the Creative Commons Attribution License, which permits use, distribution and reproduction in any medium, provided the original work is properly cited.

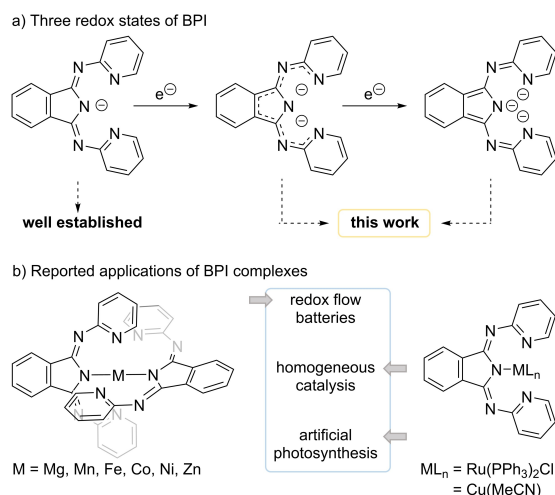


Figure 1. a) Mono-, di- and trianionic redox states of BPI. b) Examples of reported applications of complexes of the general formula $[M(\text{bpi})]$ and $[ML_n(\text{bpi})]$.^[18–21]

and paved the way to further applications, for instance, in f-element^[27] or main group chemistry.^[28] Alkali metal complexes of BPI were synthesized before in its redox-neutral state and one lithium complex^[29] was even crystallographically characterized.^[30–34] But despite some hints of the possible reductions of BPI ligands^[18,19] information on the accessibility and coordination chemistry of the reduced BPI species is, to the best of our knowledge, so far unprecedented. The lack of fundamental knowledge of these useful species prompted us to carry out a detailed study on the isolation and complete characterization of BPI-derived alkali metal complexes featuring mono-, di- and trianionic ligand entities, which benchmarks the isolated reduced redox levels of this ligand scaffold (Figure 1).

Results and Discussion

Bis(pyridylimino)isoindoline (BPI–H) is readily accessible from commercially available o-phthalonitrile and 2-amino pyridines.^[35] The pre-ligand has already been used in its deprotonated form (i.e. $[\text{BPI}]^-$) as ligand for transition metals, main group and rare earth elements.^[22] To increase the potential for future applications, the lower oxidation states of BPI were investigated in order to simplify the fine-tuning of the redox properties of metal complexes and to open gates to a new class of coordination compounds.

We started our investigations with cyclic voltammetry (CV) studies on BPI–H (1-H) and bis(3-methylpyridylimino)isoindoline ($\text{Me}_2\text{BPI-H}$, 2-H) in THF. 1-H shows a quasi-reversible reduction process at $E^0_{1/2} = -2.06$ V (vs. Fc/Fc^+). This parallels previous findings from Saha *et al.* on CV measurements in MeCN of a closely related derivative of 1-H, where the quasi-reversibility was possibly attributed to $\text{C}_{\text{pyridine}}-\text{N}$ single bond rotation on the CV time scale.^[19] In addition, Saha *et al.* reported a second irreversible reduction process of their BPI derivative centered at $E^0_{1/2} = -2.25$ V. This finding contrasts with our

results as we observed the second reduction of 1-H at $E^0_{1/2} = -2.37$ V to be quasi-reversible. The differences in reduction potential and reversibility very likely originate from the different solvent used for the CV measurements. From these findings it can be concluded that reduced BPI species might decompose in too polar solvents. Furthermore, a third reduction process was observed for 1-H at $E^0_{1/2} = -2.65$ V. This indicated deprotonation of the compound within the electrochemically active layers on CV time scale. As the anionic species were suggested to get reduced at lower potentials, the third observed reduction was expected to originate from the formation of 1^{3-} (see Supporting Information). For the dimethylated derivative 2-H in THF, this third reduction process was only barely detectable, but the first two reduction processes were observed fully reversible at $E^0_{1/2} = -2.10$ V and $E^0_{1/2} = -2.40$ V (vs. Fc/Fc^+ , Figure 2). These results indicated the possible uptake of two electrons into the conjugated π -system as well as the occurrence and potential isolation of di- and trianionic state of BPI.

Alkali metal complexes of BPI in their redox-neutral state can be synthesized by deprotonating the N–H moiety of the pre-ligand 1-H.^[29–34] As alkali metal complexes of unsubstituted BPI are highly insoluble in almost all common solvents, the derivatives of Me_2BPI were chosen for crystallographic and cyclic voltammetry investigations. $\text{Me}_2\text{BPI-Li}$ (2-Li), $\text{Me}_2\text{BPI-Na}$ (2-Na), and $\text{Me}_2\text{BPI-K}$ (2-K) were synthesized by treating 2-H with the corresponding metal hydrides in THF. While the Li and K derivatives were obtained as solvent-free samples by simple vacuum drying at ambient temperature, 2-Na is obtained as a THF adduct, which lost its coordinated solvent only by refluxing in toluene. All three compounds are soluble in polar ethers like THF or DME, but poorly soluble in apolar solvents such as hydrocarbons. Residues of coordinating THF improves the solubility in apolar solvents, which is signified by the very good solubility of $\text{Me}_2\text{BPI-Na} \cdot \text{THF}$ in toluene. The improved solubility of the methylated BPI complexes enabled the crystallization of the Li-, and K coordination compounds from supersaturated

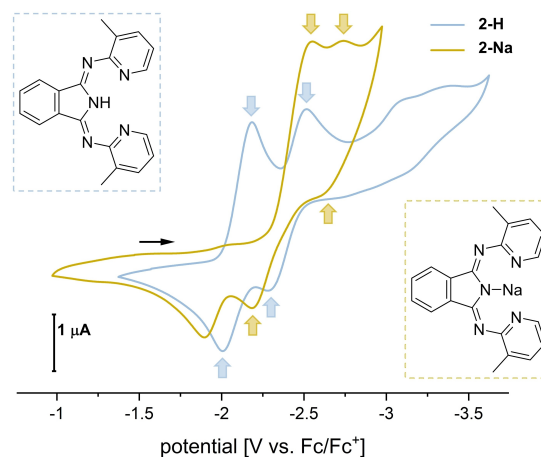


Figure 2. Cyclic voltammograms of 2-H (blue) and 2-Na (yellow) in THF under argon atmosphere using 0.01 M $[\text{NBu}_4][\text{Al}(\text{OC}(\text{CF}_3)_3)_4]$; scan rate $v = 100$ mV/s.

THF solutions. In addition, these compounds were investigated by SC-XRD (Figure 3).

The observed bond lengths along the conjugated π -system of those two complexes match the expected bond lengths of typical C–N and C–C single and/or double bonds in BPI–H pre-ligands.^[29,36] Furthermore, the C1–N2 single bond is capable of rotation, thus hampering global conjugation of the pyridine and isoindoline π -systems. This behavior is only rarely found in BPI complexes but is expected to occur if the hereby enabled metal coordination is energetically overcoming the global conjugation. Distinct from the Li complex of bis(tetrahydrochinolylimino) isoindolide,^[29] the preferred tetrahedral coordination of Li⁺ in 2-Li-THF is realized by bidentate coordination of two Me₂BPI ligands with the second pyridine ring rotating out of the BPI plane.

Cyclic voltammetry studies on 2-Li, and 2-K in THF did not yield satisfactory results, which may be due to disruptive interactions like deposition of the compounds on the electrodes surface.^[19] 2-Na instead did show two reduction processes at $E^0_{1/2} = -2.37$ V and $E^0_{1/2} = -2.65$ V (vs. Fc/Fc⁺). Therefore, the reduction processes already observed for the pre-ligand are still detectable for the alkali metal compound although cathodically shifted due to the higher electron density in the monoanionic BPI scaffold (Figure 2). Since the CV data of the pre-ligand 2-H as well as the alkali metal complex 2-Na hinted on the possible reduction of BPI, the preligand 1-H was treated with three equivalents of potassium in THF to synthesize 1-K₃. Initially, the bright yellow solution of 1-H turned into a yellow suspension, indicating the formation of insoluble 1-K through metalation

(vide supra). After several minutes, the suspension started adopting a darker color and turning finally red after stirring for one night. Stirring of the mixture for several days led to full dissolution of the former suspension. Filtration and solvent evaporation gave a black solid material, which shows good solubility in polar ethers like THF, 1,4-dioxane or DME.

NMR spectroscopic investigations in THF-*d*₈ gave only very broad signals with low intensities, which was understood as an indication of huge amounts of paramagnetic material in the substance, i.e. incomplete reduction of the BPI ligand. Nevertheless, when the reaction was carried out in the presence of 18-crown-6 (18c6) to further facilitate the reduction with elemental potassium, the reaction mixture changed colors from yellow to dark green and, finally, again to dark red within few hours. When only two equivalents of potassium were used, the green color, which is only observed if 18c6 was utilized, remained. Conducting this reaction with 2-H furnished dark green crystals from THF solution at –30 °C, which were confirmed by SC-XRD to be 2-K₂·18c6. This compound crystallizes in the monoclinic space group *P*2₁/*c* as a coordination copolymer with a “shishkebab”-like array of Me₂BPI and 18c6 moieties between the potassium ions (Figure 4). This alternation is expected to originate from a preferably balanced charge distribution along the linear polymer chain because of the different charges of both monomers, namely –2 for BPI and 0 for crown ether. Macroscopically, the different tubular polymer chains are arrayed exclusively parallel and not crossed. Distinct from 2-K, the bonds in 2-K₂ along the conjugated π -system experienced strong length alteration by reduction. For instance, the former imino C=N double bond (C2–N2) is elongated from 129.4 pm in 2-K to 135.2 pm in 2-K₂. This clearly indicates that the additional electron is populating antibonding π^* orbitals of the ligand system.

Isolated 2-K₂·18c6 is a dark green to black solid, which is well soluble in THF or DME and shows very high sensitivity to air and moisture. EPR spectroscopic investigations showed a resonance with a *g* value of 2.0066. Different hyperfine couplings were observed for all nitrogen and hydrogen atoms, but full resolution of all hyperfine couplings was hampered by line broadening. After approximate determination of the hyperfine coupling constants by quantum chemical calculations at the BP86-D3/EPR-III//BP86-D3/def2-TZVP level, the EPR spectrum was successfully simulated (Figure 5a, for details, see Supporting Information). The computed (BP86-D3/EPR-III//BP86-D3/def2-TZVP level) spin density in [Me₂BPI]²⁻ indicates that the unpaired electron is mainly localized at both exocyclic C=N bonds (computed spin density of 0.14e and 0.10e for C and N atoms, respectively, Figure 5b). This is consistent with the above-mentioned elongation of the C=N bonds from 2-K to 2-K₂, which is reflected in the Wiberg Bond Index (WBI) computed for the bare [Me₂BPI]²⁻ dianion (1.32, C=N bond length of 1.35 Å), which is close to a single bond.

The findings described above strongly suggest that the addition of a second electron should be feasible, leading to the formation of a new diamagnetic compound. Knowing that 2-K₂·18c6 is the green intermediate detected during the reaction of 2-H with excess potassium (if 18c6 is present), the second

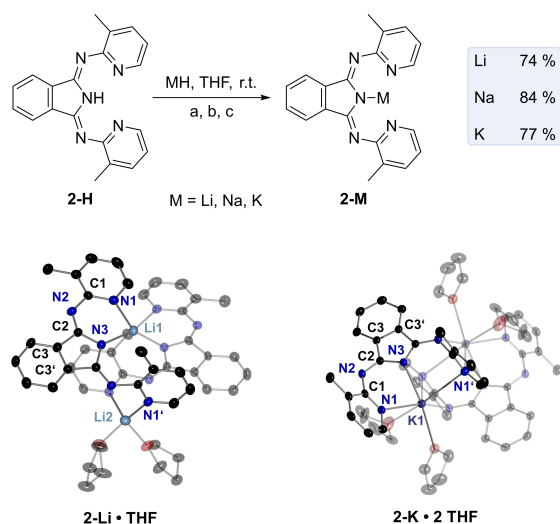


Figure 3. Top: Reaction scheme of the synthesis of Me₂BPI–M from Me₂BPI–H. a) 15.0 eq. LiH, THF, r.t., overnight, 74%; b) 1.10 eq. NaH, THF, r.t., 1 h, 84%; c) 1.05 eq. KH, THF, r.t., 1 h, 77%. Bottom: Molecular structures of 2-Li·THF and 2-K·2 THF. Thermal ellipsoids are drawn at the 30% probability level. Hydrogen atoms omitted for clarity. Selected distances, bond lengths and angles in Å and °, respectively. 2-Li·THF: N1–C1 1.330(7), C1–N2 1.388(7), N2–C2 1.298(6), C2–C3 1.495(7), C3–C3' 1.383(7), N1–Li1 2.035(9), N3–Li1 2.014(10), N1'–Li2 2.048(11); N1–C1–N2 122.6(5), C1–N2–C2 125.5(5). 2-K·2 THF: N1–C1 1.335(3), C1–N2 1.395(3), N2–C2 1.294(3), C2–C3 1.487(3), C3–C3' 1.381(3), N1–K1 2.878(2), N3–K1 2.833(2), N1'–K1 3.138(2); N1–C1–N2 119.9(2), C1–N2–C2 121.4(2).

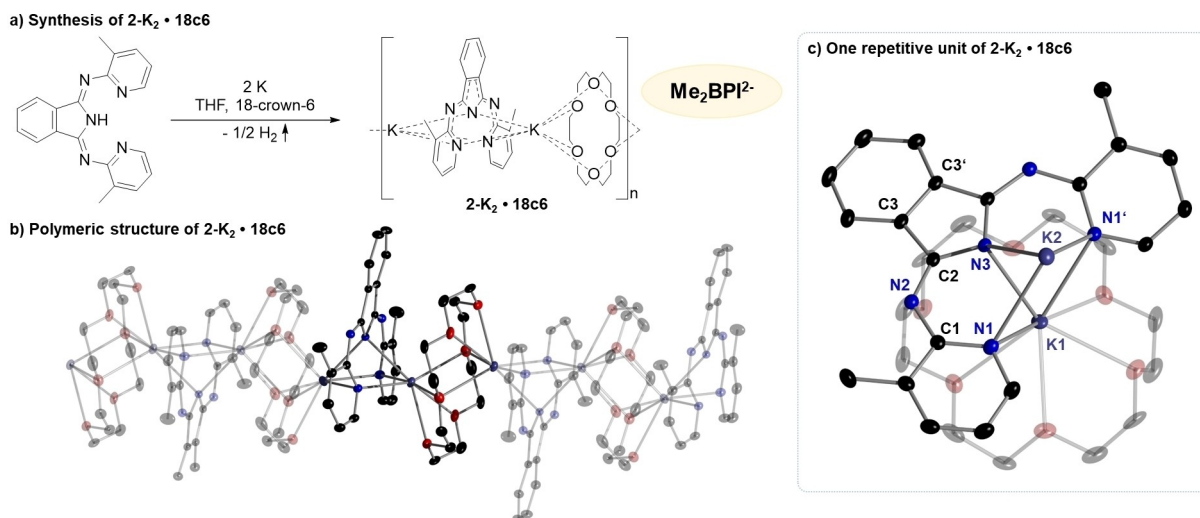


Figure 4. a) Synthesis of $2\text{-K}_2 \cdot 18\text{c6}$. 2.10 eq. K, 2.10 eq. 18-crown-6, THF, r.t., 7 d, 45%. b) Polymeric structure of $2\text{-K}_2 \cdot 18\text{c6}$ in solid state determined by SC-XRD. c) One repetitive unit of the solid-state structure of $2\text{-K}_2 \cdot 18\text{c6}$ determined by SC-XRD. Thermal ellipsoids are drawn at the 30% probability level. Hydrogen atoms and non-coordinated THF omitted for clarity. Selected distances, bond lengths and angles are given in Å and °, respectively: N1–C1 1.3630(15), C1–N2 1.3565(15), N2–C2 1.3515(15), C2–C3 1.4541(16), C3–C3' 1.4132(17), N1–K1 2.7881(10), N3–K1 2.7491(10), N1'–K1 2.8712(11), N3–K2 2.6941(10), N1'–K2 2.8867(11); N1–C1–N2 124.12(10), C1–N2–C2 124.45(10), K1–N1–K2 84.44(3).

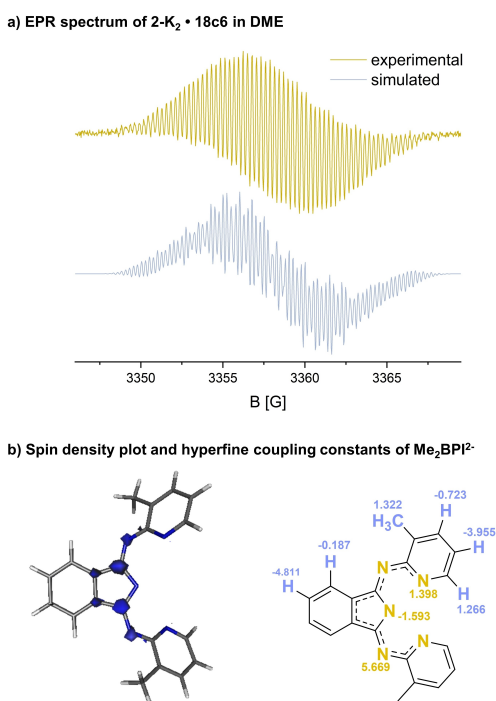


Figure 5. a) CW-EPR spectrum of $2\text{-K}_2 \cdot 18\text{c6}$ in DME (10^{-5} M, modulation amplitude: 0.02 G, 9.415471 GHz, ambient temperature, 30 scans, $g = 2.0066$). The line width was determined to $lw = 0.01252$ mT. For dependency of simulated spectrum shape to line width, see ESI; b) spin density plot (left) of $[\text{Me}_2\text{BPI}]^{2-}$ in the gas phase computed at the BP86-D3/EPR-III//BP86-D3/def2-TZVP level and hyperfine couplings constants in MHz (right) determined by simulation of the experimentally observed spectrum.

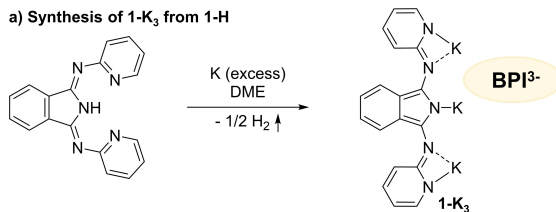
color change to red was interpreted as the result of the second electron transfer to form 2-K_3 . Unfortunately, all our attempts to isolate or characterize this species were unsuccessful. Despite

that, the isolation of a coordination compound with trianionic BPI was achieved by using the unsubstituted ligand system (i.e. lacking methyl groups in the pyridine rings). Thus, treating the parent **1-H** with an excess of potassium metal in dimethoxyethane gave dark red crystals of **1-K₃** after filtration and storage of the filtrate at -25°C . This crystalline material immediately started melting after removal from the freezer, but could still be investigated by SC-XRD. **1-K₃** crystallizes in the triclinic space group $P\bar{1}$ as a dimer with a chain of six potassium ions as connector and eight DME molecules saturating their coordination spheres above and below the molecular plane of both BPI molecules (Figure 6).

The observed “melting process” may be ascribed to the cleavage of the DME coordination to the potassium ions and the dissolution of **1-K₃** by the released DME. As previously proposed, the former double bonds of **1-H** along the conjugated backbone become much longer in **1-K₃**, while the former single bonds are strongly shortened. This is once again reflected in the computed WBIs of the key C=N bonds which are significantly lower in $[\text{BPI}]^{3-}$ (1.14, C=N bond length of 1.40 Å) than in $[\text{BPI}]^-$ (1.52, C=N bond length of 1.31 Å). Table 1 gathers the bond length variations of the key bonds upon reduction of the BPI systems.

Interestingly, the BPI ligand in **1-K₃** adopts the open form of the imino C2–N2 bond rotamer in which the NNN pincer character of the ligand is lost and the former imino C–N bond shows anti conformation. This was previously reported by Zhang et al. for a redox-neutral BPI f-element complex, but only in the solid state while the pincer-type rotamer was observed in solution.^[37] Our quantum chemical calculations at the BP86-D3/def2-TZVP level indicate that the barrier associated with the rotation around the imino C=N bond is rather low and becomes almost negligible upon reduction of the BPI ligand ($\Delta E^\ddagger =$

a) Synthesis of 1-K₃ from 1-H



b) SC-XRD of 1-K₃ · 4 DME in top view (left) and side view (right)

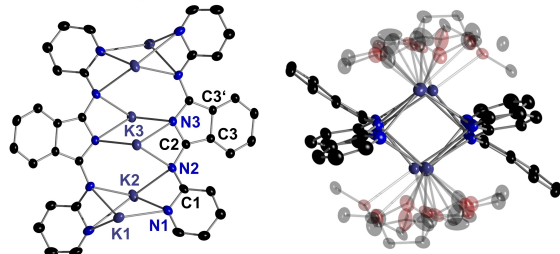


Figure 6. a) Synthesis of 1-K₃ from 1-H. 4.50 eq. K, DME, r.t., 3 d, 84%. b) SC-XRD of 1-K₃ · 4 DME in top view without showing coordinating solvent (left) and in side view (right). Hydrogen atoms and one additional uncoordinated DME molecule were omitted for clarity. Thermal ellipsoids are drawn at the 30% probability level. Selected bond lengths and angles are given in Å and °, respectively: N1–C1 1.389(4), C1–N2 1.336(4), N2–C2 1.407(4), C2–C3 1.405(4), C3–C3' 1.450(4), N1–K1 2.846(3), N1–K2 2.846(3), N2–K2 2.810(3); N1–C1–N2 115.1(3), C1–N2–C2 121.2(3).

5.2 kcal/mol, 2.2 kcal/mol and 0.8 kcal/mol, for [BPI][−], [BPI]^{2−} and [BPI]^{3−}, respectively). In addition, whereas the open-forms [BPI-iso]^{2−} and [BPI-iso]^{3−} are clearly more stable than their closed-form counterparts ($\Delta E = 5.7$ and 9.5 kcal/mol, respectively), the species involving the [BPI][−] ligand are nearly degenerate (Figure 7).

This is very likely the result of minimizing the electronic repulsion of the negative charges in the reduced systems, which are mainly located at the nitrogen atoms (Figure 7). Therefore, the open-form rotamer observed in the crystal structure involving the redox-neutral BPI reported by Zhang et al. was probably driven by more favorable metal coordination. Nevertheless, it should be noted that the ¹H NMR spectrum of isolated 1-K₃ in THF-*d*₈ did only show very broad signals between 8.00 and 5.00 ppm, which are in general shifted to higher field compared to less reduced BPI species. Although a full assignment of the observed NMR signals could not be

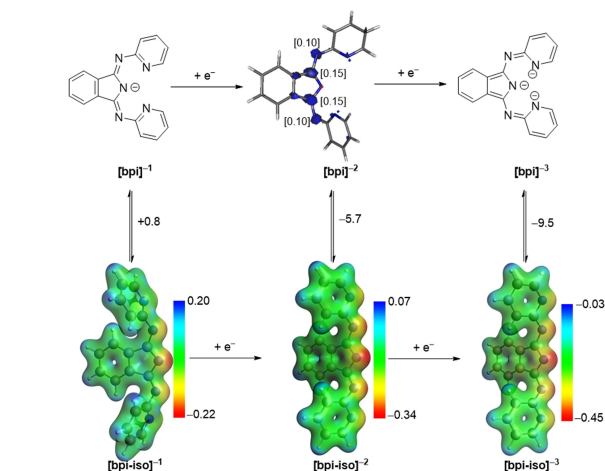


Figure 7. Computed key species and corresponding molecular electrostatic potentials for the reduction of BPI[−]. The spin density in BPI^{2−} is also shown. Energy values are given in kcal/mol. All data have been computed at the BP86-D3/def2-TZVP level.

achieved, the signals in the ¹H NMR spectra sharpened when the measuring temperature was gradually cooled down until 193 K. These findings are consistent with a dynamic C–N bond rotation on the NMR time scale as it was reported previously for related doubly reduced diamagnetic species of NILs.^[26] Conclusively, reduced BPI is a more promising candidate for applying the open coordination mode than redox-neutral BPI. In combination with the increased negative charge, the coordination mode of [BPI]^{3−} can be described as bis(amidinato)isoindolide.

Conclusions

This work established the isolation and characterization of bis(pyridylimino)isoindolide (BPI) alkali metal complexes in all three redox states. Redox-neutral Li, Na and K complexes of Me₂BPI (2) were synthesized and cyclic voltammetry studies indicated two feasible reductions of the ligand entity. The utilization of 18-crown-6 in the reduction of Me₂BPI–H (2-H)

Table 1. Comparison of bond lengths determined by SC-XRD in 2-K · 2 THF, 2-K₂ · 18c6 and 1-K₃ · 4 DME as representatives for BPI compounds in three different redox states of the ligand system.

	2-K · 2 THF	2-K ₂ · 18c6	1-K ₃ · 4 DME
d (N1-C1) [pm]	133.5	136.3	138.9
d (C1-N2) [pm]	139.5	135.7	133.6
d (N2-C2) [pm]	129.4	135.2	140.7
d (C2-C3) [pm]	148.7	145.4	140.5
d (C3-C3') [pm]	138.1	141.3	145.0
BPI oxidation state / charge	0 / -1	-1 / -2	-2 / -3

with elemental potassium furnished **2-K₂-18c6** as a paramagnetic coordination copolymer, which enabled its structural and EPR spectroscopic characterization. Reduction of the pre-ligand BPI-H (**1-H**) with an excess of potassium in DME enabled the isolation of **1-K₃** adopting the open form of the imino C₂-N₂ bond rotamer in which the NNN pincer character of the ligand is lost and the former imino C-N bond shows anti conformation. The structural features found in the solid state were corroborated by the dynamic behavior in NMR measurements and computed rotation barriers. SC-XRD studies of all obtained compounds correlated bond distances in the conjugated π -system and its degree of reduction. As alkali metal ions are suggested to be redox innocent, the herein-described redox chemistry is fully ligand controlled. Followingly, this work benchmarks the reduced oxidation states of the BPI ligand system. We are convinced that these findings will initiate a broader coordination chemistry of reduced BPI species as it was already the case for other NILs like diimines or iminopyridines.

Experimental Section

Despite the synthesis of BPI-H (**1-H**) and Me₂BPI-H (**2-H**) all manipulations were carried out under argon atmosphere within MBraun gloveboxes (MB200 G and Unilab) or using conventional Schlenk techniques. Used argon was purchased from Air liquide with a purity grade of 99.999 % and used without further drying. All manipulations concerning the compounds **2-K₂-18c6** and **1-K₃** were carried out exclusively within gloveboxes. Solid chemicals were transferred with spatulas and weighed in with an accuracy of $\pm 1\%$. If the purity of compounds was below 98 wt% the used amount was corrected by the impurity factor. Liquid chemicals were transferred by single-use Injekt® syringes by B. Braun. Filtrations were conducted by using reversible frits on the Schlenk line or by using syringe filters within the glovebox. All used chemicals were purchased from commercials and if not stated otherwise used without further purifications. Solvents were dried over Na/benzophenone or K/benzophenone, degassed by refluxing and purified by distillation. Used alkali metals were used as powder, which was obtained by cooling melted alkali metals while stirring. Ferrocene and decamethylferrocene as CV standards were sublimed before use. [nBu₄N][Al{OC(CF₃)₃]₄] was synthesized according to the literature procedure.^[38] **1-H** and **2-H** were synthesized according to the literature procedure.^[35]

NMR spectroscopy. NMR spectra were measured on an Avance Neo 400 or an Avance 300 spectrometer. ¹H and ¹³C chemical shifts are referenced to the used solvent referred to TMS.^[39]

cw-EPR spectroscopy. Continuous wave EPR spectroscopy (cw-EPR) was performed at X-band on a Bruker EMXplus spectrometer. The field was calibrated by using 2,2-diphenyl-1-picrylhydrazine (DDPH) with a *g* value of 2.0036.^[40]

CV. Cyclic voltammetry measurements were performed with an Autolab potentiostat by Metrohm (AUT40259) and an electrochemical cell within a glovebox. A freshly polished Pt disk working electrode by Metrohm, a Pt wire as counter electrode, and a Ag wire as (pseudo) reference electrode was used. As electrolyte [nBu₄N][Al{OC(CF₃)₃]₄] (0.01 M in THF) was used. Potentials were calibrated against the Fc/Fc⁺ couple by internal standardization with ferrocene or decamethylferrocene. For decamethylferrocene in THF a redox potential of -427 mV vs. the Fc/Fc⁺ couple was considered.^[41]

FT-IR. IR spectra were measured using the ATR technique (attenuated total reflection) on a Bruker Vertex 70 spectrometer in the range from 4000 cm⁻¹ to 400 cm⁻¹. The intensity of the absorption band is indicated as vw (very weak), w (weak), m (medium), s (strong), vs (very strong), and br (broad).

SC-XRD. Diffraction data were measured using a Stoe IPDS II diffractometer and graphite-monochromated MoK α (0.71073 Å) radiation or Stoe STADIVARI diffractometer and GaK α (1.34134 Å) radiation. Absorption corrections were carried out using the STOE LANA software package.^[42] Structure solution were carried out using OLEX2 1.5^[43] by dual-space direct methods with SHELXT,^[44] by full-matrix least-squares refinement using SHELXL-2014/7.^[45] All non-hydrogen atoms were refined anisotropically. The contribution of the hydrogen atoms, in their calculated positions, was included in the refinement using a riding model.

Deposition Numbers 2265570 (for **2-Li-THF**), 2265571 (for **2-K-2 THF**), 2265567 (for **2-K₂-18c6**) and 2265568 (for **1-K₃**) contain the supplementary crystallographic data for this paper. These data are provided free of charge by the joint Cambridge Crystallographic Data Centre and Fachinformationszentrum Karlsruhe Access Structures service. For further details, see section 7 of the Supporting Information.

DFT calculations. See details in the Supporting Information.

Synthesis of compounds. Detailed NMR signal assignments as well as FT-IR and elemental analysis characterization are given in the Supporting Information.

2-Li: 200 mg **2-H** (611 μ mol, 1.00 eq.) and 72.8 mg LiH (9.16 mmol, 15.0 eq.) were suspended in 10.0 mL THF and stirred at ambient temperature overnight. The suspension was filtered by syringe filter and the solvent was removed under reduced pressure. The remaining solid was dried at 10⁻³ mbar at ambient temperature for 6 hours. **2-Li** was obtained as yellow solid (145 mg, 435 μ mol, 71 %). m.p. ~260–270 °C (dec.) ¹H NMR (298 K, 300 MHz, THF-*d*₆): δ = 8.26–8.15 (m, 2H, CH), 7.85 (dd, *J* = 5.3, 3.2 Hz, 2H, CH), 7.46 (dd, *J* = 7.4, 2.0 Hz, 2H, CH), 7.40 (dd, *J* = 5.4, 3.0 Hz, 2H, CH), 6.75 (dd, *J* = 7.2, 5.1 Hz, 2H, CH), 2.48 ppm (s, 6H, CH₃). ¹³C NMR (298 K, 101 MHz, THF-*d*₆): δ = 168.5 (C_{quart.}), 161.6 (C_{quart.}), 146.0 (CH), 143.4 (C_{quart.}), 138.6 (CH), 132.1 (C_{quart.}), 129.8 (CH), 121.9 (CH), 117.6 (CH), 19.5 ppm (CH₃). ⁷Li NMR (156 MHz, THF-*d*₆): δ = 1.86 ppm.

2-Na: 200 mg **2-H** (611 μ mol, 1.00 eq.) and 16.1 mg NaH (672 μ mol, 1.10 eq.) were suspended in 8.00 mL THF and stirred at ambient temperature for one hour. The obtained suspension was filtered by syringe filter and the solvent was removed under reduced pressure. The obtained solid was dried at ~10⁻³ mbar at ambient temperature for ~4 h to give **2-Na-THF**. The solid was then dissolved in 3.00 mL toluene and heated to reflux for ~30 min while enabling the evaporation of THF which resulted in precipitation of **2-Na**. The solvent was removed under reduced pressure and the remaining solid was dried at ~10⁻³ mbar at ambient temperature for ~2 hours. **2-Na** was obtained as yellow solid (180 mg, 515 μ mol, 84 %). m.p. ~260–270 °C (dec.) ¹H NMR (298 K, 400 MHz, THF-*d*₆): δ = 8.05 (dd, *J* = 5.2, 1.9 Hz, 2H, CH), 7.79 (dt, *J* = 5.4, 2.5 Hz, 2H, CH), 7.42–7.39 (m, 2H, CH), 7.37 (dd, *J* = 5.4, 2.9 Hz, 2H, CH), 6.69 (dd, *J* = 7.2, 5.1 Hz, 2H, CH), 2.34 ppm (s, 6H, CH₃). ¹³C NMR (298 K, 101 MHz, THF-*d*₆): δ = 169.3 (C_{quart.}), 164.0 (C_{quart.}), 145.9 (CH), 143.8 (C_{quart.}), 138.1 (CH), 130.0 (C_{quart.}), 129.3 (CH), 121.4 (CH), 116.9 (CH), 19.2 ppm (CH₃).

2-K: 500 mg **2-H** (1.53 mmol, 1.00 eq.) and 64.3 mg KH (1.60 mmol, 1.05 eq.) were suspended in 8.00 mL THF and stirred at ambient temperature for one hour. The solvent was removed under reduced pressure and the residue was treated with 20.0 mL toluene. The obtained suspension was refluxed for several minutes which afforded full dissolution of all solid material. Storage of the solution

at 6 °C overnight afforded precipitation of the product. The mixture was filtered and the obtained solid was dried under reduced pressure giving **2-K** as bright green solid (429 mg, 1.17 mmol, 77%). m.p. ~260–270 °C (dec.) ¹H NMR (298 K, 400 MHz, THF-*d*₆): δ = 7.95 (d, *J* = 5.0 Hz, 2H, CH), 7.67 (s br., 2H, CH), 7.31 (dd, *J* = 10.7, 6.6 Hz, 4H, CH), 6.61 (dd, *J* = 7.3, 5.0 Hz, 2H, CH), 2.16 ppm (s, 6H, CH₃). ¹³C NMR (298 K, 101 MHz, THF-*d*₆): δ = 168.78 (C_{quart.}), 165.46 (C_{quart.}), 145.63 (CH), 143.60 (C_{quart.}), 137.60 (CH), 129.8 (C_{quart.}), 129.05 (CH), 121.32 (CH), 116.79 (CH), 18.85 ppm (CH₃).

2-K₂·18c6: 300 mg **2-H** (916 μmol, 1.00 eq.), 75.2 mg potassium metal (1.92 mmol, 2.10 eq.) and 509 mg 18-crown-6 (1.92 mmol, 2.10 eq.) were suspended with 20.0 mL THF. The mixture was stirred at ambient temperature for 7 days and subsequently filtered by syringe filter. The dark green filtrate was kept at –30 °C for 3 weeks which afforded crystallization of **2-K₂·18c6**. The solvent was removed by decantation and the obtained crystals were washed with 3.00 mL *n*-pentane to give 184 mg of **2-K₂·18c6**. Storage of the mother liquor at –30 °C for 3 months afforded another 90.0 mg of the product as crystalline material. Conclusively, **2-K₂·18c6** was obtained as black solid (274 mg, 410 μmol, 45%). m.p. ~200–210 °C (dec.) *g* value: 2.0066.

BPI-K₃: 300 mg BPI-H (1.02 mmol, 1.00 eq.) and 176 mg potassium metal (4.51 mmol, 4.50 eq.) were suspended in 25.0 mL dimethoxyethane and stirred at ambient temperature for three days. The mixture was filtered and the filtrate was stored at –25 °C overnight which afforded BPI-K₃·4DME as dark red crystals. The solution was decanted while still cold and the crystals were washed with –25 °C cold *n*-pentane. The washed crystals were dried at 10^{–3} mbar for 4 hours at ambient temperature. The product was obtained as black crystalline solid (348 mg, 0.837 mmol, 84%). m.p. not determined. ¹H NMR (193 K, 400 MHz, THF-*d*₆): δ = 7.72–7.41 (m, 2H), 6.85 (m, 2H), 6.69–6.46 (m, 2H), 6.42–6.23 (m, 2H), 6.18–5.82 (m, 2H), 5.63–5.32 ppm (m, 2H). ¹³C NMR (193 K, 101 MHz, THF-*d*₆, 193 K): δ = 166.46, 164.82, 149.80, 135.67, 134.26, 123.52, 121.12, 110.13, 101.98 ppm.

Author Contributions

Jonas Oliver Wenzel: Conceptualization, Investigation, Validation, Visualization, Writing – Original Draft Preparation. **Israel Fernández**: Investigation (Quantum chemistry), Writing – Review & Editing. **Frank Breher**: Conceptualization, Supervision, Writing – Review & Editing.

Supporting Information

Additional references cited within the Supporting Information.^[46]

Acknowledgements

This work was financially supported by the Fonds der Chemischen Industrie through a Kekulé scholarship for J.O.W. This work was partly carried out with the support of the Karlsruhe Nano Micro Facility (KNMF), a Helmholtz Research Infrastructure at Karlsruhe Institute of Technology (KIT) and we thank Prof. Dr. Dieter Fenske, Dr. Olaf Fuhr and Dr. Felix Krämer as well as Melina Dilanas and Dr. Bernhard Birenheide for help with SC-XRD. Furthermore, J.O.W.

thanks Dr. Alexander Hinz for help with CW-EPR spectroscopy and for fruitful discussions. I.F. thanks the Spanish MCIN/AEI/10.13039/501100011033 (Grants PID2019-106184GB-I00 and RED2018-102387-T) for financial support. The authors thank Nicole Klaassen for elemental analysis and Helga Berberich for NMR spectroscopic measurements. Open Access funding enabled and organized by Projekt DEAL.

Conflict of Interests

The authors declare no conflict of interest.

Data Availability Statement

The data that support the findings of this study are available from the corresponding author upon reasonable request. Supporting Information (Methods, synthesis and characterization, NMR spectra, IR spectra, cyclic voltammograms, XRD details, computational details) are provide in the ESI.

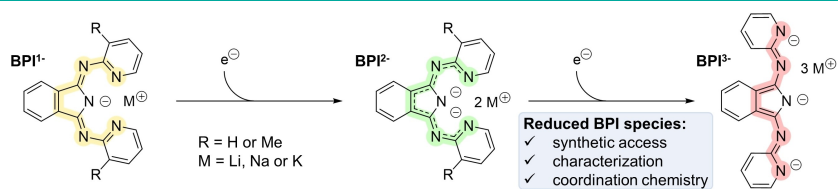
Keywords: Alkali metals · Cyclic voltammetry · N ligands · Non-innocent ligands · radical ligands

- [1] a) C. Jørgensen, *Coord. Chem. Rev.* **1966**, *1*, 164; b) W. Kaim, *Inorg. Chem.* **2011**, *50*, 9752.
- [2] a) K. Hindson, B. de Bruin, *Eur. J. Inorg. Chem.* **2012**, 340; b) K. P. Butin, E. K. Beloglazkina, N. V. Zyk, *Russ. Chem. Rev.* **2005**, *74*, 531.
- [3] a) V. Lyaskovskyy, B. de Bruin, *ACS Catal.* **2012**, *2*, 270; b) V. K. K. Praneeth, M. R. Ringenberg, T. R. Ward, *Angew. Chem. Int. Ed. Engl.* **2012**, *51*, 10228.
- [4] a) B. Ding, M. B. Solomon, C. F. Leong, D. M. D'Alessandro, *Coord. Chem. Rev.* **2021**, *439*, 213891; b) W. Kaim, G. K. Lahiri, *Coord. Chem. Rev.* **2019**, *393*, 1; c) N. A. Vázquez-Mera, F. Novio, C. Roscini, C. Bellacanzone, M. Guardingo, J. Hernandez, D. Ruiz-Molina, *J. Mater. Chem. C* **2016**, *4*, 5879.
- [5] W. Kaim, B. Schwederski, *Coord. Chem. Rev.* **2010**, *254*, 1580.
- [6] a) W. Kaim, A. Das, J. Fiedler, S. Zálaiš, B. Sarkar, *Coord. Chem. Rev.* **2020**, *404*, 213114; b) J. H. Enemark, R. D. Feltham, *Coord. Chem. Rev.* **1974**, *13*, 339; c) F. Roncaroli, M. Videla, L. D. Slep, J. A. Olabe, *Coord. Chem. Rev.* **2007**, *251*, 1903.
- [7] J. A. McCleverty, *Chem. Rev.* **2004**, *104*, 403.
- [8] A. F. Heyduk, B. J. Charette in *Comprehensive Coordination Chemistry III*, Elsevier, **2021**, pp. 650–666.
- [9] G. Periyasamy, N. A. Burton, I. H. Hillier, M. A. Vincent, H. Disley, J. McMaster, C. D. Garner, *Faraday Discuss.* **2007**, *135*, 469–88 discussion 489–506.
- [10] W. Kaim, *Dalton Trans.* **2019**, *48*, 8521.
- [11] a) A. Nakada, T. Matsumoto, H.-C. Chang, *Coord. Chem. Rev.* **2022**, *473*, 214804; b) F. F. Khan, A. D. Chowdhury, G. K. Lahiri, *Eur. J. Inorg. Chem.* **2020**, 1138.
- [12] a) M. Kumar, S. Ahmad, A. Ali, *Russ. J. Inorg. Chem.* **2022**, *67*, 1573; b) O. R. Luca, R. H. Crabtree, *Chem. Soc. Rev.* **2013**, *42*, 1440.
- [13] J. Calbo, M. J. Golomb, A. Walsh, *J. Mater. Chem. A* **2019**, *7*, 16571.
- [14] a) T. Benkó, D. Lukács, M. Li, J. S. Pap, *Environ. Chem. Lett.* **2022**, *20*, 3657; b) B. Singh, A. Indra, *Inorg. Chim. Acta* **2020**, *506*, 119440; c) N. Queyriaux, *ACS Catal.* **2021**, *11*, 4024.
- [15] J. I. van der Vlugt in *Topics in Organometallic Chemistry*, Springer Berlin Heidelberg, Berlin, Heidelberg, **2020**.
- [16] a) P. J. Chirik, K. Wieghardt, *Science* **2010**, *327*, 794; b) K. T. Sylvester, P. J. Chirik, *J. Am. Chem. Soc.* **2009**, *131*, 8772.
- [17] a) M.-C. Chang, A. J. McNeece, E. A. Hill, A. S. Filatov, J. S. Anderson, *Chem. Eur. J.* **2018**, *24*, 8001; b) S. W. Anferov, A. S. Filatov, J. S. Anderson, *ACS Catal.* **2022**, *12*, 9933.

- [18] C. S. Sevov, S. L. Fisher, L. T. Thompson, M. S. Sanford, *J. Am. Chem. Soc.* **2016**, *138*, 15378.
- [19] S. Saha, S. T. Sahil, M. M. R. Mazumder, A. M. Stephens, B. Cronin, E. C. Duijn, J. W. Jurss, B. H. Farnum, *Dalton Trans.* **2021**, *50*, 926.
- [20] T. Benkó, D. Lukács, K. Frey, M. Németh, M. M. Mócz, D. Liu, É. Kováts, N. V. May, L. Vayssieres, M. Li, J. S. Pap, *Catal. Sci. Technol.* **2021**, *11*, 6411.
- [21] A. M. Davies, Z.-Y. Li, C. R. J. Stephenson, N. K. Szymczak, *ACS Catal.* **2022**, *12*, 6729.
- [22] R. Csonka, G. Speier, J. Kaizer, *RSC Adv.* **2015**, *5*, 18401.
- [23] a) D. C. Sauer, R. L. Melen, M. Kruck, L. H. Gade, *Eur. J. Inorg. Chem.* **2014**, 4715; b) B. K. Langlotz, H. Wadepohl, L. H. Gade, *Angew. Chem. Int. Ed. Engl.* **2008**, *47*, 4670; c) J. A. Camerano, C. Sámán, H. Wadepohl, L. H. Gade, *Organometallics* **2011**, *30*, 379; d) D. C. Sauer, H. Wadepohl, L. H. Gade, *Inorg. Chem.* **2012**, *51*, 12948.
- [24] B. K. Langlotz, J. Lloret Fillol, J. H. Gross, H. Wadepohl, L. H. Gade, *Chem. Eur. J.* **2008**, *14*, 10267.
- [25] a) Y. Liu, P. Yang, J. Yu, X.-J. Yang, J. D. Zhang, Z. Chen, H. F. Schaefer, B. Wu, *Organometallics* **2008**, *27*, 5830; b) H. tom Dieck, K.-D. Franz, *Angew. Chem.* **1975**, *87*, 244; c) M. G. Gardiner, G. R. Hanson, M. J. Henderson, F. C. Lee, C. L. Raston, *Inorg. Chem.* **1994**, *33*, 2456; d) I. L. Fedushkin, A. A. Skatova, V. A. Chudakova, G. K. Fukin, *Angew. Chem.* **2003**, *115*, 3416.
- [26] H. P. Nayek, N. Arleth, I. Trapp, M. Löble, P. Oña-Burgos, M. Kuzdrowska, Y. Lan, A. K. Powell, F. Breher, P. W. Roesky, *Chem. Eur. J.* **2011**, *17*, 10814.
- [27] a) E. J. Schelter, R. Wu, B. L. Scott, J. D. Thompson, T. Cantat, K. D. John, E. R. Batista, D. E. Morris, J. L. Kiplinger, *Inorg. Chem.* **2010**, *49*, 924; b) J. Scholz, H. Görls, H. Schumann, R. Weimann, *Organometallics* **2001**, *20*, 4394.
- [28] a) P. S. Gahlaut, K. Yadav, D. Gautam, B. Jana, *J. Organomet. Chem.* **2022**, *963*, 122298; b) M. Haaf, A. Schmiedl, T. A. Schmedake, D. R. Powell, A. J. Millevolte, M. Denk, R. West, *J. Am. Chem. Soc.* **1998**, *120*, 12714; c) I. L. Fedushkin, O. V. Markina, A. N. Lukoyanov, A. G. Morozov, E. V. Baranov, M. O. Maslov, S. Y. Ketkov, *Dalton Trans.* **2013**, *42*, 7952; d) J. Wang, H. S. Soo, F. Garcia, *Commun. Chem.* **2020**, *3*, 113.
- [29] M. Kruck, D. C. Sauer, M. Enders, H. Wadepohl, L. H. Gade, *Dalton Trans.* **2011**, *40*, 10406.
- [30] K.-N. T. Tseng, J. W. Kampf, N. K. Szymczak, *Organometallics* **2013**, *32*, 2046.
- [31] B. L. Tran, M. Driess, J. F. Hartwig, *J. Am. Chem. Soc.* **2014**, *136*, 17292.
- [32] A. L. Müller, H. Wadepohl, L. H. Gade, *Organometallics* **2015**, *34*, 2810.
- [33] L. V. A. Hale, T. Malakar, K.-N. T. Tseng, P. M. Zimmerman, A. Paul, N. K. Szymczak, *ACS Catal.* **2016**, *6*, 4799.
- [34] S. K. Y. Ho, F. Y. T. Lam, A. de Aguirre, F. Maseras, A. J. P. White, G. J. P. Britovsek, *Organometallics* **2021**, *40*, 4077.
- [35] W. O. Siegl, *J. Org. Chem.* **1977**, *42*, 1872.
- [36] E. W. Y. Wong, J. S. Ovens, D. B. Leznoff, *Chem. Eur. J.* **2012**, *18*, 6781.
- [37] P. Zhang, H. Liao, H. Wang, X. Li, F. Yang, S. Zhang, *Organometallics* **2017**, *36*, 2446.
- [38] I. Raabe, K. Wagner, K. Guttsche, M. Wang, M. Grätzel, G. Santiso-Quiñones, I. Crossing, *Chem. Eur. J.* **2009**, *15*, 1966.
- [39] G. R. Fulmer, A. J. M. Miller, N. H. Sherden, H. E. Gottlieb, A. Nudelman, B. M. Stoltz, J. E. Bercaw, K. I. Goldberg, *Organometallics* **2010**, *29*, 2176.
- [40] L. van Gerven, J. Talpe, A. van Itterbeek, *Physica* **1967**, *33*, 207.
- [41] I. Noviadri, K. N. Brown, D. S. Fleming, P. T. Gulyas, P. A. Lay, A. F. Masters, L. Phillips, *J. Phys. Chem. B* **1999**, *103*, 6713.
- [42] J. Koziskova, F. Hahn, J. Richter, J. Kožíšek, *Acta Chim. Slov.* **2016**, *9*, 136.
- [43] O. V. Dolomanov, L. J. Bourhis, R. J. Gildea, J. A. K. Howard, H. Puschmann, *J. Appl. Crystallogr.* **2009**, *42*, 339.
- [44] G. M. Sheldrick, *Acta Crystallogr. Sect. A* **2015**, *71*, 3.
- [45] G. M. Sheldrick, *Acta Crystallogr. Sect. C* **2015**, *71*, 3.
- [46] a) V. Barone in *Recent Advances in Density Functional Method Part I* (Ed.: D. P. Chong), World Scientific Publ. Co., Singapore, **1996**; b) C. Gonzalez, H. B. Schlegel, *J. Phys. Chem.* **1990**, *94*, 5523; c) S. Grimme, J. Antony, S. Ehrlich, H. Krieg, *J. Chem. Phys.* **2010**, *132*, 154104; d) F. Weigend, R. Ahlrichs, *Phys. Chem. Chem. Phys.* **2005**, *7*, 3297; e) A. D. Becke, *Phys. Rev. A* **1988**, *38*, 3098; f) J. P. Perdew, *Phys. Rev. B* **1986**, *33*, 8822; g) Gaussian 09, Revision D.01, M. J. Frisch, G. W. Trucks, H. B. Schlegel, G. E. Scuseria, M. A. Robb, J. R. Cheeseman, G. Scalmani, V. Barone, G. A. Petersson, H. Nakatsuji, X. Li, M. Caricato, A. Marenich, J. Bloino, B. G. Janesko, R. Gomperts, B. Mennucci, H. P. Hratchian, J. V. Ortiz, A. F. Izmaylov, J. L. Sonnenberg, D. Williams-Young, F. Ding, F. Lipparini, F. Egidi, J. Goings, B. Peng, A. Petrone, T. Henderson, D. Ranasinghe, V. G. Zakrzewski, J. Gao, N. Rega, G. Zheng, W. Liang, M. Hada, M. Ehara, K. Toyota, R. Fukuda, J. Hasegawa, M. Ishida, T. Nakajima, Y. Honda, O. Kitao, H. Nakai, T. Vreven, K. Throssell, J. A. Montgomery, Jr., J. E. Peralta, F. Ogliaro, M. Bearpark, J. J. Heyd, E. Brothers, K. N. Kudin, V. N. Staroverov, T. Keith, R. Kobayashi, J. Normand, K. Raghavachari, A. Rendell, J. C. Burant, S. S. Iyengar, J. Tomasi, M. Cossi, J. M. Millam, M. Klene, C. Adamo, R. Cammi, J. W. Ochterski, R. L. Martin, K. Morokuma, O. Farkas, J. B. Foresman, and D. J. Fox, Gaussian, Inc., Wallingford CT, **2016**.

Manuscript received: May 26, 2023
Revised manuscript received: June 14, 2023
Accepted manuscript online: June 16, 2023

RESEARCH ARTICLE



This work reports on the synthesis and characterization of alkali metal complexes of BPI and Me₂BPI in reduced oxidation states. CV, EPR and XRD studies revealed detailed infor-

mation about the unknown lower oxidation states of BPI, which is well-established in coordination chemistry but so far only in its redox-neutral state.

*J. O. Wenzel, Prof. Dr. I. Fernández, Prof. Dr. F. Breher**

1 – 9

Synthesis and Characterization of Bis(pyridylimino)isoindolide Alkali Metal Complexes in Three Redox States

